JCEC
THE JOURNAL OF ENGINEERING AND EXACT SCIENCES

OPEN ACCESS

The Journal of Engineering and Exact Sciences – jCEC, Vol. 09 N. 08 (2023)
journal homepage: https://periodicos.ufv.br/jcec
eISSN: 2527-1075
ISSN: 2446-9416

New experimental investigation of 3D defects propagation in mortar under tension loading

Article Info:
Article history: Received 2023-05-05 / Accepted 2023-10-04 / Available online 2023-10-04
doi: 10.18540/jcecvl9iss8pp16580-01e

Mohamed Guesmi
ORCID: https://orcid.org/0000-0002-1826-2485
FST, University of Djelfa, Djelfa, 17000, Algeria
E-mail: guesmi82@gmail.com
Kamel Guesmi
ORCID: https://orcid.org/0000-0002-3492-8339
2CReSTIC, University of Reims, Reims, 51100, France
E-mail: guesmi01@univ-reims.fr

Abstract
Among the construction materials, the mortar is the weakest component, especially against tensile loading and cracking. We propose in this paper an experimental study of the propagation of 3D internal defects in the mortar for different dosages and their effects on the tensile strength of the mortar. We start by deter- mining the tensile strength of a non-cracked specimen for five different dosages. After that, as our first contribution, we calculate the tensile strength and the critical Stress Intensity Factor SIF for the different dosages. Then, as our second contribution, we investigate the effect of the defects shape on the stability limit. Finally, we consolidate, through a comparative study, the obtained experimental results with the numerical ones.
Keywords: Mortar, defects, Brazilian test, Tensile strength, Critical Stress Intensity Factor, Stability limit.

1. Introduction

Among the most commonly used materials, in civil engineering, are mortar and concrete. They are so popular thanks to their durability, strength, and affordability. The mortar's main disadvantage is its low tensile strength, making it subject to defects and reducing, therefore, its strength and durability. Defects can be caused by several factors such as tensile loading, plastic shrinkage, and aggressive chemical reactions with the environment (Zamba *et al*., 2023)

Defects have a major impact on the mechanical behavior of cementitious materials such as mortars and concrete. These materials are heterogeneous and have complicated microstructures that can be modeled differently at different scales. Defects are initiated from the Nano-scale and grow to the micro, and macro scales. The research efforts, in this area, are divided into two groups; one of them tries to model the fracture process to understand the birth reasons for those defects, the failure mechanisms, and even predicts the growth of defects. The objective, in this case, is to fix the problem locally or innovate new materials more resistant to defects or completely free of them. The second research group is focused on experimental studies to analyze the growth of defects and develop strengthening techniques for the damaged zone. For example, experimental characterization of the mortar defects reinforced with multiwall carbon nanotubes was proposed in (Gdoutos *et al*., 2022).

Several strategies for healing the defects are experimented on using Epoxy Resin, Car- bon Fibre Reinforced Polymers, Bonded Overlays, Micro bacteria, and Electrochemical solution (Bano *et al*., 2023). In 2023 (Zhu *et al*., 2023), an experimental and numerical study of the defect growth in specimens under radial impact load provided a reference to evaluate the cemented rock under a

dynamic load. A Micro-encapsulated bacterial spore was employed as an additive substance to self-repairing the shrinkage defect in mortar (Nuaklong *et al*., 2023). This solution accelerated the rate of defect healing area in the early stage and showed that the use of bacterial spores has high potential use to seal the shrinkage defect. In 2019, a study investigated the use of vibrothermography to detect defects in concrete parts, and the obtained experimental results demonstrated that this inspection technique could suitably detect concrete defects (Jia *et al*., 2019).

A mesoscale model of mixed-mode fracture in concrete was developed using the finite element method. In addition, the defect propagation process was analyzed by Xiong and Xiao (2019) while taking into consideration the aggregates' effects. A three-dimensional numerical method was proposed in Zhang *et al*. (2023) to simulate the propagation process of the mode-I local defect in the concrete and the results showed that the local defect propagates alongside the thickness' direction and parallel to the upper bound-areas. A numerical simulation of mixed-mode defect propagation in concrete using the scaled boundary finite element method (SBFEM) and cohesive defect approach was studied in Alrayes *et al*. (2023). The proposed method investigated defect growth propagation and dam- age accumulation for cyclic loading within the SBFEM framework. In the same area, we previously developed a numerical analysis of brittle propagation of 3D defects with different forms using the weight function method (Guesmi *et al*., 2010, and Hachi *et al.*, 2012), and we found that defects under tensile loading, always propagate to a stable circular form regardless of their initial form.

This paper provides an experimental study of pre-added internal defect propagation in mortar. The influence of the cement dosages and the defect shapes on the tensile strength and stress intensity factor will be analyzed and compared to our previous numerical results.

This paper is organized as follows: it starts with some notions about mortar and the reasons for choosing it, then the used experimental method and equipment in the present study, followed by the determination of the dimensions of the defect, specimens, and the process of defect creation on fresh mortar and we finish with an analysis of the obtained results and their interpretations.

2. Notions about mortar

Mortar is a well-studied and well-perfected mixture of cement, fine sand, and water. Sometimes, we add other elements to liquefy, slow or accelerate the hardening process. The mortar has great importance in the field of masonry and plastering works and is also considered the most fragile constituent of concrete. For the aforementioned reasons, mortar was chosen as the subject of our study. In addition, it has greater brittleness and homogeneity compared to concrete which is more suitable for numerical and experimental studies on compression. It should also be pointed out that testing this material using, especially, the direct tensile test is a delicate issue and gives very scattered results and important errors between numerical results and experimental ones (Neville, 2011) and this is the main reason for choosing the splitting test in our present study. The wide dispersion of the experimental results prompted civil engineers to standardize all mortar components: water, sand, and cement, as well as all dosing and mixing standards and conditions. Indeed, mortar is affected by several parameters including:

- Type of cement.
- Cleanliness and humidity of sand, and its mineral origin and grain size.
- Cleanliness of water, chemical elements such as salt, and impurities.
- Mixing conditions.
- Dosage of the three elements: water, sand, and cement.
- Hardening time.
- Additives.

Any imperfection in those parameters can initiate defects from the Nano to the micro- scale. The mortar is chosen in the present study due to the following properties:

- Mortar is the weakest constituent of concrete under tensile loading and cracking in Mode-I.
- Mortar has sufficient brittleness and homogeneity compared to concrete, which
- Makes it suitable for numerical study assumptions.
- Despite the very delicate experimental creation of internal defects in this material, but is still possible during the casting operation.

3. Materials and methods

3.1. Materials

The materials utilized are sourced locally and are readily found in the Algerian market.

Cement: Our research employs Portland cement, specifically a CPA CEM I / 52.5 grade cement produced at the M'sila factory. Table 1 provides the cement's physical characteristics, while Table 2 presents its chemical and mineralogical analysis.

Table 1 – Physical properties of cement.

Properties	CEM I/B
Specific density (kg/m3)	3016
Apparent density (kg/m3)	1125
Fineness (cm2/g)	3905

Table 2 – Chemical and mineralogical composition of cement.

Mineralogical composition (%)								
C3S		C2S		C3A		C4AF		
61,35		14,74		7,05		11,85		
Chemical composition (%)								
SiO2	CaO	Al2O3	Fe2O3	MgO	SO3	Na2O	K2O	LOI
20,77	61,36	5,2	3,42	1,68	2,81	0,12	0,78	1,78

Sand: The sand utilized is sourced from the Oued M'zi region, situated to the north of Laghouat town, and it is classified as alluvial sand with a particle size range of 0/5. It has a fineness modulus of Mf = 2.35.

Mixing water: The water used is clean and potable tap water.

3.2. Splitting tests (Brazilian test)

In the splitting test, the mortar cylinder is fixed horizontally in special equipment as shown in Figure 1a to put it between the press platens, and the load is increased until indirect tensile failure occurs. This appears as a splitting along the cylinder's vertical diameter. If the load is applied along the cylinder height, an element on the vertical diameter of the cylinder, as depicted in Figure 1b, is subjected to the compressing stress (1) as mentioned in Neville (2011):

$$\sigma_C = \frac{2P}{\pi LD}\frac{D^2}{r(D-r)} - 1 \quad (1)$$

with a horizontal tensile stress expressed by:

$$\sigma_{tr} = \frac{2P}{\pi LD} \quad (2)$$

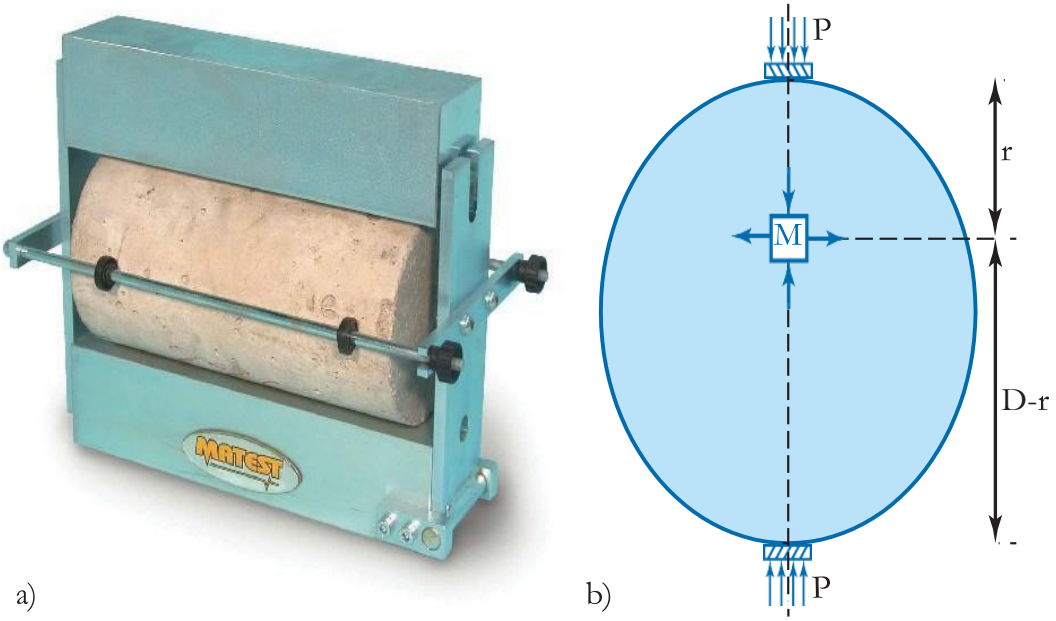

Figure 1 – Splitting test a) Test Equipment. b) Section view of the specimen.

Where P is the compression force, L is the specimen length, D the cylinder diameter, r and D-r are the distances of the element M from the load application points.

In practice, the specimen is remedied by inserting thin strips of a distribution material such as plywood between the cylinders and the press platens. Without strips, the measured resistance is usually 8% lower on average. The standard ASTM C 496–04 (2017) specifies that the plywood strips are of 3 mm thick and 25mm wide. British standard BS 1881, Part 117:1983 (2017) specifies the hardwood strips of 4mm thick and 15mm wide. French standard NF.P 18-408:1981 (1981) specifies 1cm-wide, 4mm-thick strips of Okoume plywood.

The splitting test is easy to perform and gives more homogeneous results than other tensile tests. The tensile strength measured in the splitting test appears to be fairly close (within 5% to 12%) to the concrete strength determined by direct tensile testing according to O'cleary and Byrne (1960).

Hydraulic press machine: This machine is an ordinary Hydraulic press used mostly in civil engineering laboratories. It is fitted with a digital display and control buttons for the parameters adjustment and showing the effort expended by the press. The MATEST press shown in Figure 2 is available from the National Laboratory of Housing and Construction (Djelfa subdivision), and it has a capacity of 1500 KN.

Figure 2 – Hydraulic press MATEST.

4. Defects' and specimens' dimensions

Our previous study dealt with several direct tensile experiment (Guesmi, 2010), which resulted in no difference in fracture stress between cracked and non-cracked specimens, despite that the cracked specimens prepared to break at the defect plane but it did not. We deduced, in the direct tensile experiment, that the fracture is induced by tensile stress and not because of the pre-added defects. This obligates us to use the splitting test. It provides, indeed, better results and the closest ones to the numerical results (Guesmi *et al*., 2010). defect geometry was also well studied and carried out according to an empirical relationship of the stress intensity factor SIF deduced from some previous studies of internal defects contained in a finite media (Jenq and Shah, (1984) as illustrated in Figure 3. For concrete, the critical Stress Intensity Factor SIF at room temperature according to Jenq and Shah (1984) is approximately$K_{IC} = 1M\ Pa.m^{1/2}$, and the mortar tensile strength according to our previous study (Guesmi, 2010) is approximately σ_{tr} = 1.2MPa.

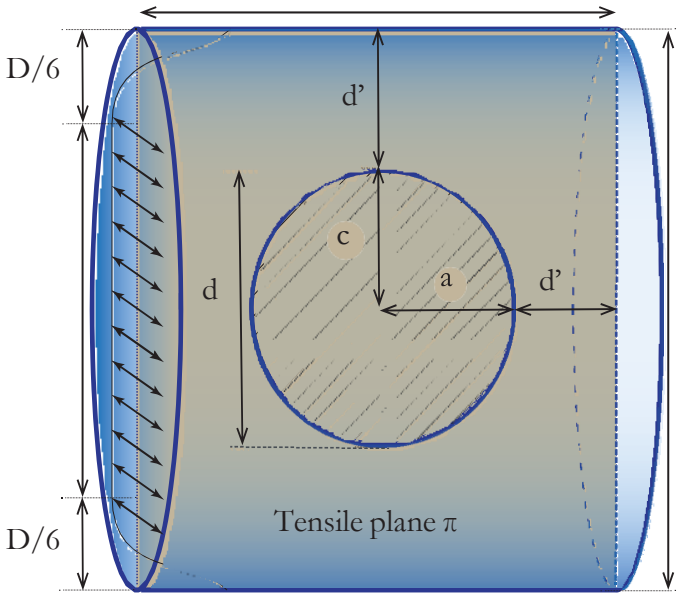

Figure 3 – Descriptive sketch of the defect and the specimen dimensions.

According to Toribio *et al*. (2017) and Newman *et al*. (1984), the empirical expression of critical SIF in mode-I for an elliptical internal defect in the finite medium (specimen) shown in Figure 3 is

$$K_{Ic} = \sigma_{tr} F \sqrt{\frac{\pi a_c}{Q}} \tag{3}$$

Where the factor $F = (M_1 + M_2\lambda^2 + M_3\lambda^4)\, f_w$ and constants $\lambda = \frac{d}{D}, M_1 = 1,\ M_2 = 0.05/(0.11 + (a/c)^{1.5}),\ M_3 = 0.29/(0.23 + (a/c)^{1.5}),\ Q = 1 + 1.464(a/c)^{1.65}$.
For circular defect, $a = c$ we have $M_2 = 0.05/1.11, M_3 = 0.29/1.23, Q = 2.464$, and the factor is given by Newman *et al*., (1984) $fw = \sqrt{\sec\left(\frac{\pi c}{L}\sqrt{2a/t}\right)}$. We choose the ratio 2a/D = 9/10, and D = L to obtain reasonable and feasible dimensions for the specimen and to facilitate defect setting.

Using the values of previous constants as: $d = 2a/D = 0.9, M1 = 1, M2 = 0.045, M3 = 0.235, fw = 2.096, F = 2.496$ in the empirical expression (1) to find the critical radius defect a_c

$$a_c = \frac{\pi K_{Ic}^2}{(2\sigma_{tr}F)^2} = 0.0874m = 8.74cm \tag{4}$$

With the specimen diameter:

$$D = \frac{10(2a_C)}{9} = 19.433 = 8.74cm \tag{5}$$

We adopt the feasible dimensions for the specimen $L = D = 19.5\, cm$, and for defect diameter $d = 2a_c = 17.5cm$.

5. Defects' and specimen's preparing

To create a defect in the specimen, very thin objects of different materials are placed in the specimens. They can be pieces of very smooth, rigid plastic paper covered with a film of oil as shown in Figure 4a. They will not deform during gluing and will not stick to the mortar after hardening. The defects have precise, pre-defined shapes and should be inserted in the center of the specimen during the casting process as shown in Figure 3. The plastic molds, for the splitting test, are made from plastic PV C200 with an internal diameter equal to $D = 19.5\, cm$ as depicted in Figure 4b.

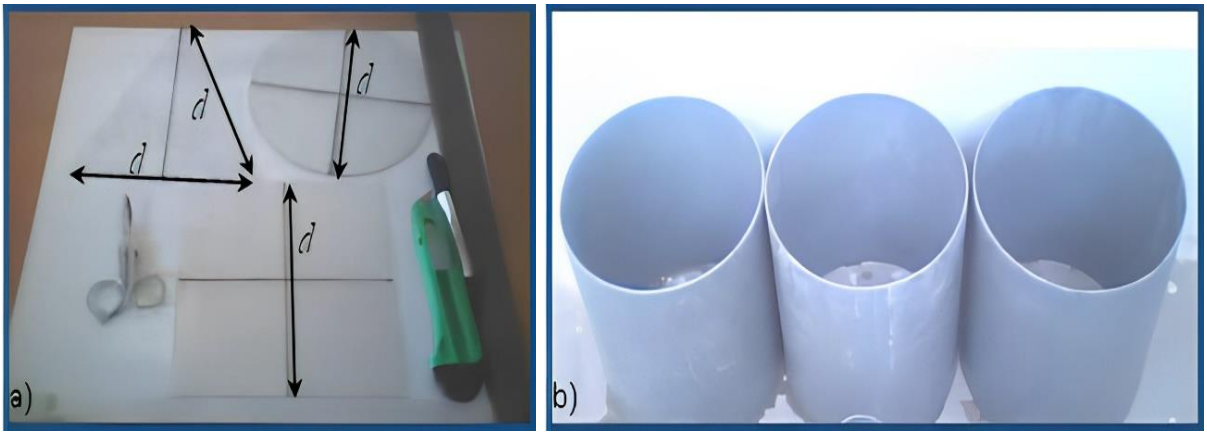

Figure 4 – Equipment for the splitting test. a) Plastic Shapes, b) Plastic molds.

The setting rules are:

- For each type of defect and dosage, three samples are taken to ensure the reliability of the experiment.
- Set the water/cement ratio to W/C = 0.5, except in the case of dosing 100 kg/m^3
- we set W/C = 1.2
- Casting mortar into specimens on 4 or 5 layers.
- To compact well the mortar during casting, we opted for the vibration, as the consistency of the used mortar is firm.
- Specimens are tested at the 7-day curing age.

5.1 Non-cracked specimens

The non-cracked specimens were prepared with 5 dosages 100 kg/m^3, 200 kg/m^3, 300kg/m^3, 400 kg/m^3, 500 kg/m^3, for a reason to see the variation in tensile strength as a function of dosage, and also these specimens can be considered as control specimens.

5.1 Cracked specimens

After the first layer of mortar has been applied, the plastic shape was put on the diagonal plane of the mold, respecting the distances between the defect and the inner boundaries of the mold (Figure 3)

Subsequent layers of mortar are then applied and compacted without touching or modifying the location or the shape of the plastic film (defect). The specimens were distributed as follows:

- For dosages 400 kg/m^3 we prepared test specimens with circular, square, and equilateral triangular defects. This is to determine the influence of the defect shape on the dimensionless stability limit and also to check the conformity of our numerical results presented by Guesmi *et al*., (2010).

- For dosages 100 kg/m^3, 200 kg/m^3, 300kg/m^3, 400 kg/m^3, 500 kg/m^3, specimens with circular defects were prepared and subjected to splitting test, to calculate the critical SIF (toughness) of the mortar for those dosages.

6. Results and discussions

Three parties, in this section, will be presented. Starting with the determination of tensile strength for non-cracked specimens with five cement dosages and considering it as a control test. Then the critical stress intensity factor SIF of cracked specimens with circular defects with the same dosages will be discussed. We finish this section by analyzing the effect of the defect shape on the dimensionless stability limit with a qualitative comparison with our numerical results.

6.1 Mortar tensile strength

Splitting tests are carried out on the specimens without defects and for different dosages. The obtained results are illustrated in Figure 4.

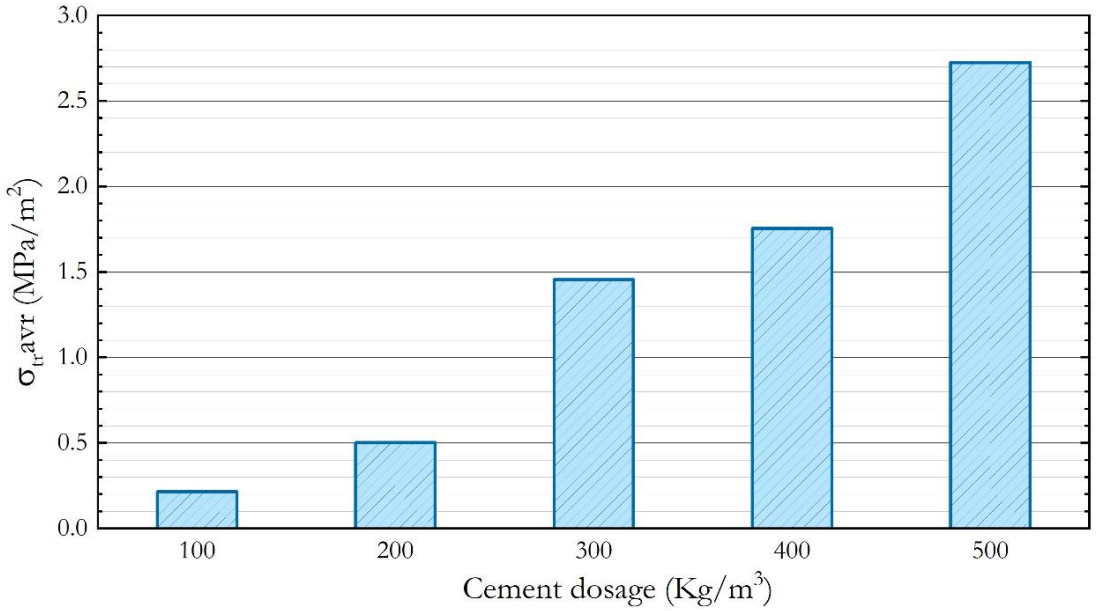

Figure 5 – Tensile stress for different dosages.

Inspecting the Figure 4 we can say:

- It is obvious that tensile strength is proportional to cement dosage in a nonlinear way. This is due to the respect of the ratios: water/cement and cement/sand.
- We observe that there is some dispersion of results between the three tests for each dosage due to the influencing factors cited in the previous section.

6.2 Critical stress intensity factor (toughness)

The splitting test is carried out on specimens with circular defects and for different dosages. The critical SIF KIC in mode-I is calculated using the empirical equation (3). Figure 6 shows the critical SIF KIC for different dosages.

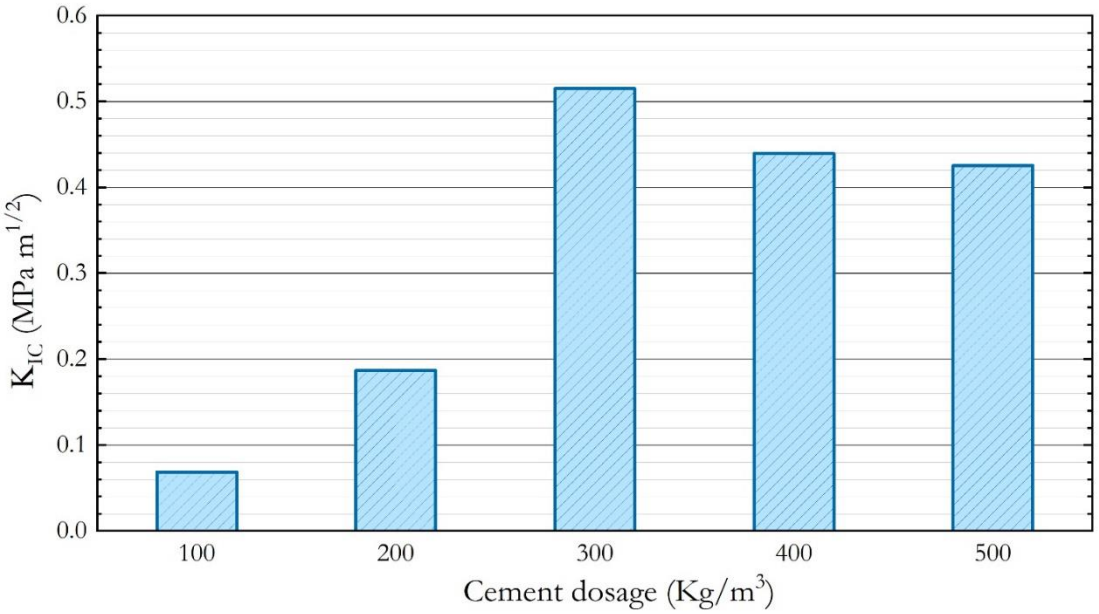

Figure 6 – Critical SIF for different dosages.

From Figure 6 we notice that SIF is proportional to the cement dosage till the value KIC = 0.6 MPa.m$^{1/2}$ corresponding to dosage 300 kg/m^3, then it becomes inversely proportional. This can be explained by the presence of very small defects in tensile plane π and connecting with circular defects at the dosage 400 kg/m^3 and 500 kg/m^3 before crushing. This is the result of the increase in the quantity of cement and water according to the sand, which generates shrinkage during hardening, accompanied by internal tensile stresses. Hence, the relationship between critical SIF and the cement dosage is nonlinear.

6.3 Defect shape effect and numerical results

The control specimens and pre-cracked specimens after the splitting test are shown in Figure 7. At first sight, the pre-cracked specimens are split in the tensile plane π regardless of the defect shape as shown in Figures 7 a, b, and c. It is a predictable result for the reason that the defects are pre-dimensioned to force the specimens to crash by the effect of the defect, and also because the defects are pre-added at the plane π that is subject to the greatest tensile load. Additionally, the control specimen was not split perfectly in the tensile plane π, as depicted in 7d, which proves that the specimen is crashed by the effect of the tensile strength and there is no defect oriented to the fracture trajectory.

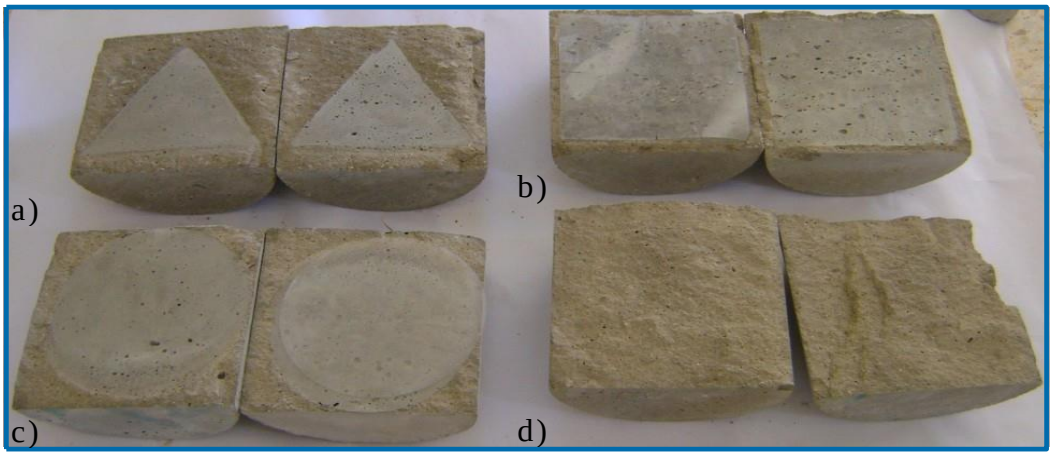

Figure 7 – Specimens after splitting. a) triangular defect, b) rectangular defect, d) circular defect, c) control specimen.

The experimental and numerical expressions of the dimensionless stability limit are respectively:

$$\sigma_{exp} = \frac{\sigma_{tr}\sqrt{d}}{K_{IC}} \tag{6}$$

$$\sigma_{num} = \frac{\sigma_{tr}\sqrt{d}}{K_{max}} \tag{7}$$

where d is the diameter of the defect, KIC is the critical stress intensity factor calculated from the experimental data, $Kmax$ the maximum stress intensity factor calculated by Guesmi *et al*. (2010) using the tensile stress σ_{tr}. Figure 8 illustrates the experimental and numerical dimensionless stability limits. From Figure 8, we have the following interpretations:

- The values of the dimensionless stability limits of all cracked specimens are very small compared to the control spacemen which illustrates the strong effect of the added defects regardless of their shapes.

- We deduce that the square defect is the most dangerous, followed by the circular defect, and finally the triangular one. This order of danger by defect shape is confirmed by the numerical results presented by Hachi *et al.* (2012). This fact can be explained by the defects surfaces where we have: $S_{square} = 3.63\,cm^2$, $S_{circle} = 27.49\,cm^2, S_{triangle} = 15.31\,cm^2$ with the dimensionless stability limit that decreases with the increase of the defect surface as confirmed by Figure 8.

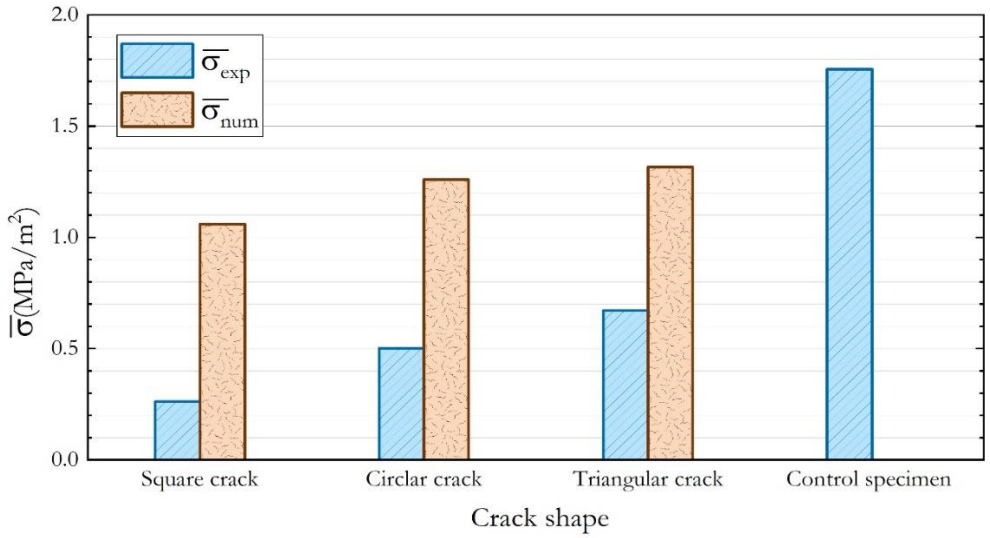

Figure 8 – **Qualitative comparison between experimental and numerical dimensionless stability limits.**

7. Conclusion

In this paper, indirect tensile using splitting tests were carried out on the weakest constituent of concrete, which is the mortar. We obtained, through this study, a range of conclusions that can be summarized as follows: i) Determination of the tensile strength of mortar for different dosages has shown that cement dosage has a proportional effect on the mortar strength. ii)Determination of critical SIF of pre-cracked mortar for different dosages has also shown a proportional relationship until the dosage 300 kg/m^3. The latter can be considered as the optimum dosage since it corresponds to the maximum critical toughness, and therefore maximum resistance to cracking. iii)defect geometry influences the dimensionless stability limit, therefore, the brutal fracture. This confirms our previous numerical studies and gives a very clear idea of the risk of brutal fracture and the defect-shape effect.

Acknowledgements
I would like to extend my sincerest appreciation and deep gratitude to the dedicated technicians and engineers at the Djelfa subdivision of the National Laboratory of Housing and Construction in Algeria.

References

Alrayes, O., K¨onke, C., Hamdia, K.M. (2023). A numerical study of crack mixed mode model in concrete material subjected to cyclic loading. *Materials*, *16*(5), 19. doi: https://doi.org/10.3390/ma16051916

ASTM C 496–04. (2017). “British Standard Testing Concrete. Part 117. Method for Determination of Tensile Splitting Strength”, UK. British Organization for Standardization.

ASTM C 496–04. (2017). “Standard Test Method for Splitting Tensile Strength of Cylindrical Concrete Specimens”, International Organization for Standardization, USA.

Bano, S., Jaiswal, G., Kumar, R., Tiwari, A., Karthikeyan, M. (2023). Experimental study on the crack repair techniques of concrete structures: A case study. *National Conference on Structural and Geotechnical Engineering*. 1273 012006. doi: https://doi.org/10.1088/1757-899X/1273/1/012006
doi : https://doi.org/10.3389/feart.2022.1037756

Gdoutos, E., Konsta-Gdoutos, M. (2022). Fracture mechanics characterization of mortar nanocomposites reinforced with carbon nanotubes. *Вестник СПбГУ. Математика. Механика. Астрономия* 9(67), 3, 452–463. doi: https://doi.org/10.21638/spbu01.2022.306

Guesmi, M. (2010). *Modélisation des fissures planes de forme quelconque dans des structures 3d par la méthode des fonctions de poids avec aperçu expérimental sur la fissuration du mortier*. PhD thesis, University of Djelfa, Algeria.

Guesmi, M., Hachi, B.E.-K., Badaoui, M., Rechak, S. (2010). Modélisation des fissures planes de forme quelconque dans des structures 3d par la méthode des fonctions de poids a incrémentation numérique. *Congrès National de la Physique et de ces Applications* 58, 6.

Hachi, B.E.-K., Guesmi, M., Haboussi, M. (2012). Modeling of planar embedded cracks of arbitrary shape under no uniform mode I loadings. *Applied Mechanics and Materials* 232, 568–572.doi: https://doi.org/10.4028/www.scientific.net/AMM.232.568

Jenq, Y.S., Shah, S.P. (1984). Two parameters fracture model for concrete. *Journal of eengineering Mechanics*, 111(10). doi: https://doi.org/10.1061/(ASCE)0733-9399(1985)111:10(1227

Jia, Y., Tang, L., Xu, B., Zhang, S. (2019). Crack detection in concrete parts using vibrothermography. *Journal of Nondestructive Evaluation* 38, 11 doi: https://doi.org/10.1007/s10921-019-0562-0

Neville, A.M. (2011). *Properties of Concrete*. Pearson Education Limited, England, UK.

Newman, J.C., Raju, I.S. (1984). Stress-intensity factor equations for cracks in three- dimensional finite bodies subjected to tension and bending loads. *NASA Technical Reports Server*. Langley Research Center.

NF P 18-408. (1981). "Norme Francaise: Beton-essai de Fondage", French Organization for Standardization.

Nuaklong, P., Jongvivatsakul, P., Phanupornprapong, V., Intarasoontron, J., Shahzadi, H., Pungrasmi, W., Thaiboonrod, S., Likitlersuang, S. (2023). Self-repairing of shrinkage crack in mortar containing microencapsulated bacterial spores. *Journal of Materials Research and Technology* 23, 3441–3454. doi : https://doi.org/10.1016/j.jmrt.2023.02.010

O'cleary, D.P., Byrne, G.J. (1960). Testing concrete and mortar in tension. *Engineering* 11, 384–5

Toribio, J., Matos, J.-C., Gonzalez, B. (2017). Aspect ratio evolution in embedded, surface, and corner cracks in finite-thickness plates under tensile fatigue loading. *Applied Sciences* 7(7):746. doi: https://doi.org/10.3390/app7070746

Xiong, X., Xiao, Q. (2019) Meso-scale simulation of concrete based on fracture and interaction behavior. *Applied Sciences*, 9(15). doi : https://doi.org/10.3390/app9152986

Zamba, D.D., Mohammed, T.A., Getu, Y.M., Tufa, D.H., Demiss, B.A. (2023). Experimental investigation on self-healing efficiency of mortar with bacillus subtilis and bacillus cereus. *Advances in Materials Science and Engineering*, 24, 11. doi:: https://doi.org/10.1155/2023/9399101

Zhang, J., Wang, S., Dong, W. (2023). Three-dimensional numerical study on mode-I local crack propagation of concrete considering boundary effect. *Theoretical and Applied Fracture Mechanics* 125(14). doi :https://doi.org/10.1016/j.tafmec.2023.103856

Zhu, C.-X., Sun, J.-X., G., J., Wang, F.-E. (2023). Experimental and numerical research of crack propagation process and energy dissipation law of grouting specimens under radial impact load. *Frontiers in Earth Science* 10, 1037756.